1-29-2005

Vertical Heat and Constituent Transport in the Mesopause Region by Dissipating Gravity Waves at Maui, Hawaii (20.7°N), and Starfire Optical Range, New Mexico (35°N)

Alan Z. Liu
Embry Riddle Aeronautical University - Daytona Beach, liuz2@erau.edu

Chester S. Gardner

Vertical heat and constituent transport in the mesopause region by dissipating gravity waves at Maui, Hawaii (20.7°N), and Starfire Optical Range, New Mexico (35°N)

Alan Z. Liu and Chester S. Gardner

Department of Electrical and Computer Engineering, University of Illinois at Urbana-Champaign, Urbana, Illinois, USA

Received 28 April 2004; revised 19 August 2004; accepted 9 November 2004; published 29 January 2005.

[1] Vertical heat flux profiles induced by dissipating gravity waves in the mesopause region (85–100 km altitude) are derived from Na lidar measurements of winds and temperatures at Maui (20.7°N, 156.3°W), Hawaii, and compared with earlier results from Starfire Optical Range (SOR, 35.0°N, 106.5°W), New Mexico. The heat flux profile at SOR has a single downward maximum of 2.25 ± 0.3 K m/s at 88 km, while the profile at Maui has two downward maxima of 1.25 ± 0.5 K m/s and 1.40 ± 0.5 K m/s at 87 and 95 km, respectively. The common maximum below 90 km can be attributed to high probability of convective instability. Comparison of the horizontal wind shear suggests that the second maximum at 95 km at Maui may be associated with dynamic instability. The measured Na flux and predicted Na flux based on measured heat flux at Maui agree well, further confirming earlier findings using SOR data. The dynamical flux of atomic oxygen estimated from the heat flux is smaller at Maui compared with that at SOR, but both are comparable to or larger than the eddy flux. The results also suggest that weaker gravity wave dissipation at Maui may cause two opposite effects on the energy balance in the mesopause region, a reduced cooling from heat transport and reduced chemical heating from atomic oxygen transport.

Citation: Liu, A. Z., and C. S. Gardner (2005), Vertical heat and constituent transport in the mesopause region by dissipating gravity waves at Maui, Hawaii (20.7°N), and Starfire Optical Range, New Mexico (35°N), *J. Geophys. Res.*, *110*, D09S13, doi:10.1029/2004JD004965.

1. Introduction

[2] Gravity waves in the mesopause region have large amplitudes and often experience strong dissipation due to various mechanisms such as convective and dynamic instabilities, nonlinear wave-wave and wave-mean flow interactions, and critical layer filtering [*Hodges*, 1969; *Hines*, 1970; *Lindzen*, 1981]. Dissipating gravity waves transport heat and momentum, and can significantly influence the mean thermal and wind structure [*Holton*, 1983; *Garcia and Solomon*, 1985; *Hamilton*, 1996; *Alexander and Holton*, 1997]. *Walterscheid* [1981] showed theoretically that dissipating gravity waves have a net downward heat flux. Dissipating gravity waves can also impart a net downward flux to the minor constituents. This net flux is different from the eddy diffusion which is a mixing process associated with turbulence. *Liu and Gardner* [2004] have shown that dynamical flux is comparable in importance to the eddy flux in transporting atomic oxygen in the region of strong gravity wave dissipation.

[3] Because nondissipating gravity waves have zero heat flux, direct measurement of the heat flux can provide the information about gravity wave dissipation [*Gardner et al.*, 2002]. However, measuring heat flux is difficult because it is a small quantity compared to instantaneous point variances of temperature and wind [*Tao and Gardner*, 1993; *Gardner and Yang*, 1998]. Long time data averaging is necessary to reduce the uncertainty from these large variances. To include the effects of typical gravity waves, measurements with high temporal and spatial resolutions (~5 min and ~1 km vertical) and high signal-to-noise ratio are also necessary.

[4] The University of Illinois Na wind/temperature lidar is coupled to the 3.7 m telescope at Maui Space Surveillance Complex (MSSC) on top the Haleakala mountain in Maui, HI (20.7°N, 156.3°W), and has been making high resolution wind and temperature measurements since Jan 2002. The large power aperture product of this system provides measurements with high signal-to-noise ratio, which makes it possible to directly measure the gravity wave heat flux. At Maui, a total of over 100 hr of observation have been obtained through May 2004. Before moving to Maui, the lidar was installed at Starfire Optical Range (SOR, 35.0°N, 106.5°W), NM and used to make similar measurements, which yielded over 400 hours of observations. In this paper, we report the analysis of heat flux based on the lidar measurements made at Maui and compare the results with those from SOR. SOR is located at midlatitudes while Maui is in the subtropics. Comparison of the heat fluxes at these two locations can provide insights into the differences of gravity wave dissipation at these two latitudes that may be associated with differences in the

0148-0227/05/2004JD004965$09.00

thermal and wind structure. One objective of this paper is to identify these differences and understand their consequences. We will also compare the atomic oxygen flux by dissipating gravity waves following *Liu and Gardner* [2004]. The atomic oxygen density is important in the mesopause region because it is involved in chemical reactions that have strong influence to the thermal balance in this region.

2. Data Analysis

[5] The Na lidar is located on top of the Haleakala mountain in Maui, HI. It is coupled to the 3.7 m AEOS (Advanced Electro-Optic System) telescope and used to make nighttime observations of temperature, Na density, and all three wind components between about 80 and 105 km altitude. A total of over 100 hours of measurements were conducted on 27 different nights from January 2002 to May 2004. The lidar and telescope were pointed sequentially at zenith (Z) and 30° off zenith to the north (N), south (S), east (E), and west (W) in the sequence NEZSWZ. At each direction the backscatter profiles were accumulated for 90 s. The raw line-of-sight (LOS) wind, temperature, and Na density data were derived from each profile at a range resolution of 480 m and were then binned to 960 m to further reduce the uncertainty due to photon noise. At this resolution the mean RMS error between 85 and 100 km for temperature, LOS wind, and relative Na density are about 2 K, 1.6 m/s, and 0.7%, respectively. The resulting Na, temperature, and wind data include gravity wave perturbations with vertical wavelengths larger than 2 km and observed periods longer than 6 min.

[6] In this analysis, only the zenith profiles are used to calculate the vertical fluxes. They provide simultaneous measurements of Na density, vertical wind and temperature in the same atmospheric volume. The heat flux is simply the covariance between the vertical wind perturbation and the potential temperature perturbation, $\langle w'\theta'\rangle$, where the prime denotes gravity wave perturbation and the angle brackets denote ensemble averaging. For most gravity waves, the Bousinnesq approximation is valid so the heat flux can be approximated as $\langle w'T'\rangle$. Similarly, the Na flux is $\langle w'\rho'_{Na}\rangle$, where ρ'_{Na} is wave-perturbed Na number density. For each night, the temporal and vertical means are subtracted from the Na density, vertical wind and temperature to obtain ρ'_{Na}, w' and T', respectively. The vertical heat flux $\langle w'T'\rangle$ and Na flux $\langle w'\rho'_{Na}\rangle$ are then calculated for each night and the results from all nights are averaged. Variances of ρ'_{Na}, w' and T' from each night are also calculated. They are used to derive the uncertainty of the estimated heat and Na fluxes (see *Gardner and Yang* [1998] and *Liu and Gardner* [2004] for details). The heating rate due to heat flux convergence is

$$-\frac{1}{\overline{\rho}}\frac{\partial\overline{\rho}\langle w'T'\rangle}{\partial z} = -\frac{\partial\langle w'T'\rangle}{\partial z} - \langle w'T'\rangle\frac{d\ln\overline{\rho}}{dz} = -\frac{\partial\langle w'T'\rangle}{\partial z} + \langle w'T'\rangle\left(\frac{g}{RT}+\frac{d\ln\overline{T}}{dz}\right). \quad (1)$$

Here the mean temperature $\overline{T}$ is the average temperature of all nightly mean temperatures.

[7] The SOR data were processed using similar procedures. The mean RMS errors between 85 and 100 km for temperature, LOS wind and relatively Na density at SOR are about 1.3 K, 1 m/s, and 0.4%, respectively. Overall, the SOR data has a higher signal-to-noise ratio and smaller uncertainty than the Maui data. All fluxes were smoothed with a 4 km full width Hamming window.

3. Heat Flux

[8] The heat flux at Maui and SOR are shown in Figure 1. The heat flux is mostly downward at both locations. This is consistent with theoretical predictions [*Walterscheid*, 1981; *Weinstock*, 1983]. Because a much longer data set is available at SOR, the uncertainty is smaller than at Maui. The heat flux at Maui has two peaks of -1.25 ± 0.5 K m/s and -1.40 ± 0.5 K m/s at 87 and 95 km, respectively. The heat flux at SOR has a single peak of -2.25 ± 0.3 K m/s at about 88 km. This difference suggests that gravity wave dissipation at these two locations happen at different altitudes and with different magnitudes. At Maui, there are two regions that gravity waves are likely to dissipate but their magnitude is smaller than at SOR. At SOR, the dissipation is confined to the region between 85 and 92 km. The heating rates (Figures 1c and 1d) associated with the dynamical flux have maximum cooling of over 50 K/day at both Maui and SOR, a significant value compared with radiative effects. The gravity wave dissipation is therefore an important factor to the thermal balance in the mesopause region.

[9] *Gardner et al.* [2002] showed that the region of large downward heat flux at SOR between 85 and 92 km coincides with low static stability. Because this region is just below the mesopause throughout the year, the temperature lapse rate is large compared with the region above 95 km. Gravity waves that propagate into this low static stability region are more likely to experience instability and strong dissipation. At Maui, while there is some difference in the temperature structure compared to SOR [*Chu et al.*, 2005], there is no significant difference in static stability at SOR and Maui below 95 km. Convective instability alone cannot explain this second peak in the heat flux profile at Maui. Besides convective instability dynamic instability can also lead to gravity wave dissipation. Dynamic instability is associated with strong wind shear and is characterized by the Richardson number, Ri, defined as

$$Ri = \frac{N^2}{S^2} = \frac{N^2}{(du/dz)^2+(dv/dz)^2}, \quad (2)$$

where N^2 is Brunt-Vaisala frequency squared, u and v are zonal and meridional wind, respectively, and S is the total wind shear. Dynamic instability is likely to occur when $Ri <$ 1/4. For a typical value of $N^2 = 4 \times 10^{-4}$ s^{-2}, this corresponds to $S > 40$ m/s/km. At Maui, because of strong diurnal tides, the horizontal wind shear is very strong.

[10] Figure 2a shows the total wind shear averaged from all nights for both Maui and SOR. There are two maxima in the total wind shear at Maui, one at 88 km and the other at 95 km, both are at the same altitudes where the downward heat flux is maximum. The total wind shear at SOR decreases with increasing altitude reaching a minimum at

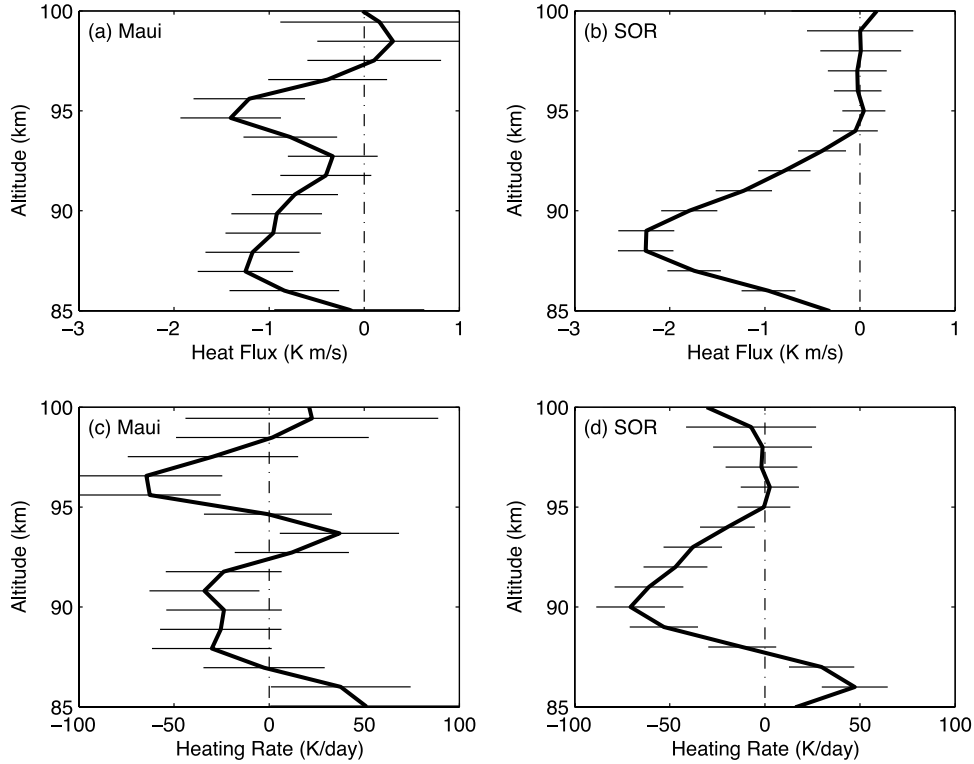

Figure 1. Heat flux derived from Na lidar vertical wind and temperature measurements at (a) Maui, HI, and (b) SOR, NM, and the corresponding heating rates at (c) Maui and (d) SOR. Error bars are shown as thin lines.

96 km, then increases above. The local maximum at 88 km at Maui has similar magnitude to that at SOR while the one at 95 km is much higher than at SOR. Even though the difference in the mean wind shear at the two sites is not very large, the difference in the probability of wind shear greater than 40 m/s/km can be quite large. Figure 2b shows the percentage of data points at each altitude that is larger than 40 m/s/km, i.e., likely to be dynamically unstable. Between 87 and 95 km, the percentage at Maui is larger than at SOR. Just below 95 km, the percentage at Maui has a peak value of over 11%, more than twice as large as the minimum of SOR percentage just above 95 km (<5%). This suggests that the stronger gravity wave dissipation at 95 km at Maui may be related to higher probability of dynamic instability associated with stronger wind shear. The other large dissipation region around 88 km at both Maui and SOR is likely due to higher probability of convective instability.

4. Na and Atomic Oxygen Fluxes

[11] *Liu and Gardner* [2004] showed that the dynamical flux of any atmospheric constituent associated with dissipating gravity waves could be estimated from the measured heat flux given the mean background distribution of the constituent:

$$DF = \langle w'\rho' \rangle \approx \frac{1}{\gamma - 1} \frac{\overline{\rho}}{\overline{T}} \left(1 - \frac{\gamma}{1 - \Gamma_e/\Gamma_a} \frac{H}{H_\rho} \right) \langle w'T' \rangle, \quad (3)$$

where γ is the ratio of specific heats, Γ_e is atmospheric lapse rate, Γ_a is adiabatic lapse rate, $\overline{T}$ is background

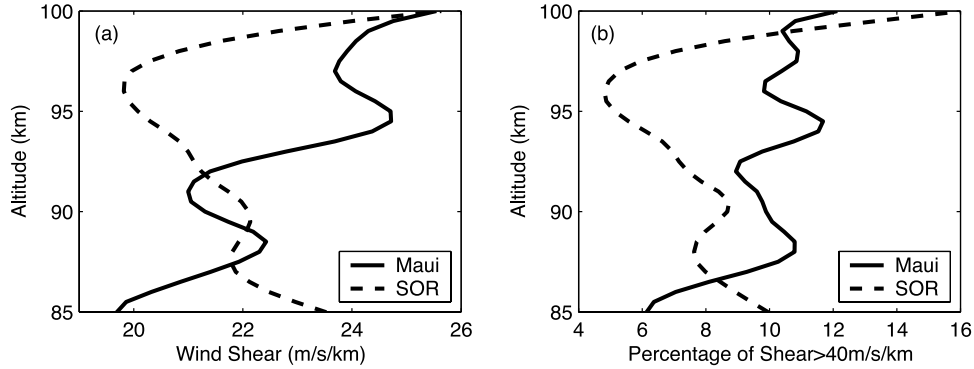

Figure 2. (a) Mean total horizontal wind shear at Maui and SOR. (b) Percentage of data that have total wind shear larger than 40 m/s/km.

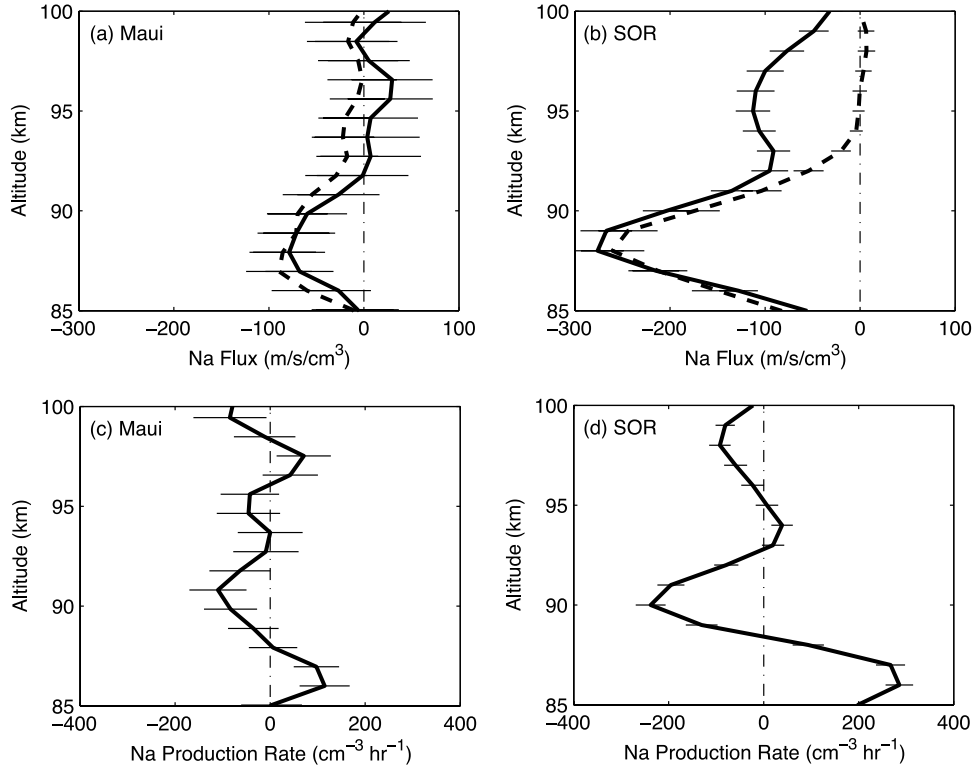

Figure 3. Na flux due to dissipating gravity waves calculated from the measured Na density and vertical wind measurements (thick solid lines), and predicted from heat flux measurements (dashed lines) at Maui (a) and SOR (b). Na production rate calculated from measured Na flux at (c) Maui and (d) SOR. Error bars are shown as thin lines.

temperature, $\bar{\rho}$ is the background constituent number density and ρ' is its perturbation. H and H_ρ are scale heights of background atmospheric density and constituent density, respectively.

[12] The dynamical fluxes of Na at both locations are shown in Figures 3a and 3b, together with the Na flux that is predicted by using the measured heat flux in (3). The measured Na flux and predicted dynamical flux agree reasonably well at all altitudes at Maui and below 92 km at SOR. This again supports the idea that measured heat flux can be used to estimate constituent flux because they are both associated with the same wave dissipation mechanism [*Liu and Gardner*, 2004]. Figure 3 also shows that the Na flux at Maui is smaller than that at SOR, likely due to less gravity wave dissipation. The dynamical flux causes a net loss of Na that peaks at around 90 km, at the rate of 100 $cm^{-3}hr^{-1}$ at Maui and over 200 $cm^{-3}hr^{-1}$ at SOR.

[13] Atomic oxygen plays important roles in the upper mesosphere and lower thermosphere (MLT). Above the mesopause, solar UV radiation absorbed by molecular oxygen and ozone are stored as chemical energy in atomic oxygen. This energy is released through exothermic chemical reactions such as $O + O + M \rightarrow O_2 + M$ and $O + O_3 \rightarrow O_2 + O_2$ [*Mlynczak and Solomon*, 1995; *Riese et al.*, 1994]. The distribution of atomic oxygen is therefore an important factor in the energy budget in the MLT region. Because the atomic oxygen has a long life time (several days) at mesopause heights, the transport of atomic oxygen is also an important energy transport mechanism. The atomic oxygen flux is commonly calculated based on eddy diffusion. As shown in the work of *Liu and Gardner* [2004], the dynamical transport of atomic oxygen by dissipating gravity waves can be as important as eddy transport in the mesopause region.

[14] The transport of atomic oxygen by dissipating gravity waves can be estimated using (3) and the measured heat flux at Maui and SOR. The mean atomic oxygen profile is obtained from the annual mean local midnight profile in MSIS-00 at Maui and SOR (Figure 4). The predicted dynamical flux of atomic oxygen is shown in Figure 5. The dynamical flux has a similar shape to the heat flux, with two downward maxima at Maui and one maximum at SOR. For comparison, two estimates of eddy flux are also shown with eddy diffusion coefficients of 50 m^2/s and 100 m^2/s. The estimate of eddy diffusion coefficient in the mesopause region varies from a few tens m^2/s [*Garcia and Solomon*, 1994; *Chabrillat et al.*, 2002; *Kaufmann et al.*, 2002; *Plane*, 2004] to a few hundred m^2/s [*Hocking*, 1990]. We chose the two values to represent this range of estimates. At Maui, the eddy flux of atomic oxygen is comparable to the dynamical flux at all altitude. At SOR, the dynamical flux is larger than the eddy flux at its peak near 89 km and smaller above 92 km. Compared with SOR, the larger eddy flux at Maui is due to a steeper atomic oxygen profile between 85 and 97 km (Figure 4). At both locations, the dynamical flux is significant and can have a large impact on the distribution and vertical transport of atomic oxygen, especially in the

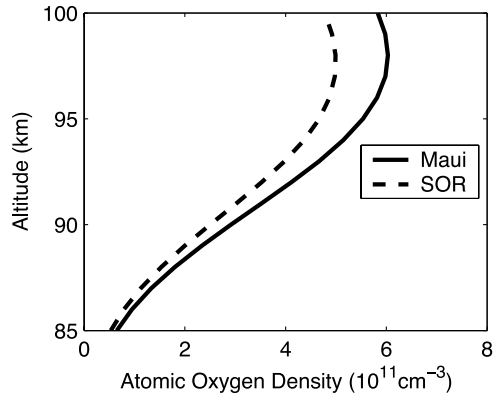

Figure 4. Annual mean atomic oxygen profile at midnight local time at Maui (solid line) and SOR (dashed line) based on MSIS-00. These O profiles and the measured heat flux profiles were used to calculate the dynamic flux of atomic oxygen shown in Figure 5.

region where strong wave dissipation occurs [*Gardner et al.*, 2002]. The production rate due to the dynamical flux of atomic oxygen (Figures 5c and 5d) shows a net loss of 10^{10} cm^{-3}hr^{-1}, a significant value compared with the mean atomic oxygen density. Because both dynamical and eddy fluxes depend on the mean atomic oxygen profile, which can vary with time and location, the actual fluxes of atomic oxygen need to be calculated based on realistic background atomic oxygen profiles.

5. Summary and Discussion

[15] We used Na lidar measurements of vertical wind and temperature to estimate the heat flux and Na flux and to predict the atomic oxygen flux in the mesopause region between 85 and 100 km. The results from Maui and SOR are compared. The annual mean heat flux at Maui, HI has two downward maxima at 87 km and 95 km, with values at -1.25 ± 0.5 K m/s and -1.40 ± 0.5 K m/s, respectively. At SOR, the heat flux has a single peak at 88 km with a value of -2.25 ± 0.3 km/s. The cooling rate associated with the heat flux has peak values exceeding 50 K/day at both sites.

[16] The heat flux profile at Maui is quite different from that at SOR. Because heat flux is a measure of gravity wave dissipation, the double peak of heat flux at Maui suggests that there are two regions, centered around 87 km and 95 km, where gravity waves experience strong dissipation. At SOR, the heat flux peaks only in the lower part of this 85–100 km region. *Gardner et al.* [2002] explained this as due to the high probability of convective instability because the annual mean temperature profile shows a large lapse rate in the region below 90 km. At Maui, the mean temperature structure is similar because it is mainly determined by the height of the mesopause. Convective instability therefore cannot explain the double peak structure in the heat flux. By examining the horizontal wind shear, we found that the wind shear is larger

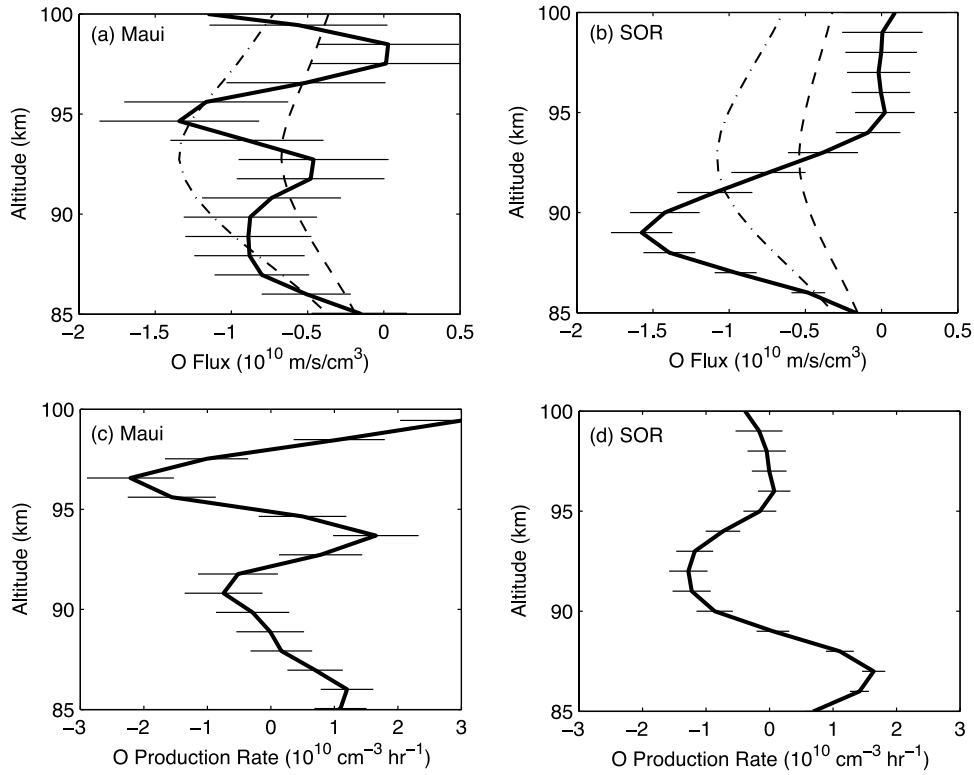

Figure 5. Atomic oxygen flux due to dissipating gravity waves (solid lines) and eddy diffusion at (a) Maui and (b) SOR. The dynamic flux was estimated from the lidar measured heat flux. The eddy flux was calculated with an eddy diffusion coefficient of 100 m^2/s (dash-dotted lines) and 50 m^2/s (dashed lines). Atomic oxygen production rates due to the predicted dynamical flux for (c) Maui and (d) SOR.

above 95 km at Maui compared with SOR. There is higher probability of dynamic instability in this region at Maui than at SOR. The enhanced heat flux at 95 km at Maui compared to SOR appears to be associated with the enhanced probability of dynamic instability in this region at Maui.

[17] The lidar measurements were also used to directly calculate the Na flux. The Na flux is also predicted from the heat flux, according to *Liu and Gardner* [2004], and it agrees well with the measurement. The Maui Na flux predictions provide further evidence that the measured heat flux profile can be used to estimate minor constituent fluxes due to dissipating gravity waves. These results were used to estimate the dynamical fluxes of atomic oxygen by the dissipating gravity waves based on the heat flux measurements. They have similar structures to the heat flux, with two downward maxima at Maui and one at SOR. The dynamical flux is comparable to the eddy flux at Maui. At SOR, the dynamical flux is larger than the eddy flux in the region of strong wave dissipation.

[18] In the comparison of thermal structure between Maui and SOR, *Chu et al.* [2005] found that the mesosphere inversion layer (MIL) is weaker at Maui than at SOR. This may be attributed to the weaker gravity wave dissipation, and therefore weaker downward flux of atomic oxygen. The atomic oxygen is associated with several chemical reactions in this region that converts solar energy to chemical heating. This chemical heating can contribute to the formation of MIL. The dissipating gravity waves transport oxygen downward, so they play an important role in chemical heating. When the dissipation is weaker, the chemical heating may also be weaker, leading to a weaker MIL.

[19] However, the heat flux by dissipating gravity waves has a net cooling effect in most of the region. This is opposite to the chemical heating due to atomic oxygen flux. In most modeling studies of this atmospheric region, the effects of dissipating gravity waves are not included. The effects of heat transport and chemical heating are both significant but may be opposite. The net effect can only be quantified with more detailed modeling studies.

[20] Directly measuring heat flux due to gravity wave dissipation is a challenging task. Because the heat flux is a small quantity compared to the large instantaneous point variance of wind and temperature, the measurement has large uncertainty. This uncertainty can only be reduced by averaging the heat flux estimates over long time periods. The lidar measurement at SOR provides relatively good estimate of the heat flux profile with low uncertainty because it was derived from over 400 hours of observations compared to only 100 hours at Maui. As additional wind and temperature measurements are accumulated at Maui, the uncertainties in the heat flux measurements will decrease.

[21] **Acknowledgments.** The authors gratefully acknowledge Xinzhao Chu, George Papen, Chirantan Mukhopadhyay, Jeff Bruggemann, and Jim Sherman for their contributions in acquiring the Na lidar data at Maui. The support provided by the staff at the Maui Space Surveillance Complex are appreciated. This work was sponsored by NSF grants ATM-00-03198 and ATM-03-38425.

References

Alexander, M. J., and J. R. Holton (1997), A model study of zonal forcing in the equatorial stratosphere by convectively induced gravity waves, *J. Atmos. Sci.*, *54*, 408–419.

Chabrillat, S., G. Kockarts, D. Fonteyn, and G. Brasseur (2002), Impact of molecular diffusion on the CO_2 distribution and the temperature in the mesosphere, *Geophys. Res. Lett.*, *29*(15), 1729, doi:10.1029/2002GL015309.

Chu, X., C. S. Gardner, and S. J. Franke (2005), Nocturnal thermal structure of the mesosphere and lower thermosphere region at Maui, Hawaii (20.7°N), and Starfire Optical Range, New Mexico (35°N), *J. Geophys. Res.*, *110*, D09S03, doi:10.1029/2004JD004891.

Garcia, R. R., and S. Solomon (1985), The effect of breaking gravity waves on the dynamics and chemical composition of the mesosphere and lower thermosphere, *J. Geophys. Res.*, *90*(D2), 3850–3868.

Garcia, R. R., and S. Solomon (1994), A new numerical model of the middle atmosphere: 2. Ozone and related species, *J. Geophys. Res.*, *99*(D6), 12,937–12,952.

Gardner, C. S., and W. Yang (1998), Measurements of the dynamical cooling rate associated with the vertical transport of heat by dissipating gravity waves in the mesopause region at the Starfire Optical Range, New Mexico, *J. Geophys. Res.*, *103*(D14), 16,909–16,926.

Gardner, C. S., Y. Zhao, and A. Z. Liu (2002), Atmospheric stability and gravity wave dissipation in the mesopause region, *J. Atmos. Sol. Terr. Phys.*, *64*(8–11), 923–929, doi:10.1016/S1364-6826(02)00047-0.

Hamilton, K. (1996), Comprehensive meteorological modeling of the middle atmosphere: A tutorial review, *J. Atmos. Sol. Terr. Phys.*, *58*, 1591–1627.

Hines, C. O. (1970), Eddy diffusion coefficients due to instabilities in internal gravity waves, *J. Geophys. Res.*, *75*(19), 3937–3939.

Hocking, W. K. (1990), Turbulence in the region 80–120 km, *Adv. Space Res.*, *10*, 153–161.

Hodges, R. R. (1969), Eddy diffusion coefficients due to instabilities in internal gravity waves, *J. Geophys. Res.*, *74*, 4087–4090.

Holton, J. R. (1983), The influence of gravity wave breaking on the circulation of the middle atmosphere, *J. Atmos. Sci.*, *40*(10), 2497–2507.

Kaufmann, M., O. A. Gusev, K. U. Grossmann, R. G. Roble, M. E. Hagan, C. Hartsough, and A. A. Kutepov (2002), The vertical and horizontal distribution of CO_2 densities in the upper mesosphere and lower thermosphere as measured by CRISTA, *J. Geophys. Res.*, *107*(D23), 8182, doi:10.1029/2001JD000704.

Lindzen, R. S. (1981), Turbulence and stress owing to gravity wave and tidal breakdown, *J. Geophys. Res.*, *86*, 9707–9714.

Liu, A. Z., and C. S. Gardner (2004), Vertical dynamical transport of mesospheric constituents by dissipating gravity waves, *J. Atmos. Sol. Terr. Phys.*, *66*(3–4), 267–275, doi:10.1016/j.jastp.2003.11.002.

Mlynczak, M. G., and S. Solomon (1995), A detailed evaluation of the heating efficiency in the middle atmosphere, *J. Geophys. Res.*, *98*(D6), 10,517–10,541.

Plane, J. M. C. (2004), A new time-resolved model of the mesospheric Na layer: Constraints on the meteor input function, *Atmos. Chem. Phys. Discuss.*, *4*, 39–69.

Riese, M., D. Offermann, and G. Brasseur (1994), Energy released by recombination of atomic oxygen and related species at mesopause heights, *J. Geophys. Res.*, *99*(D7), 14,585–14,594.

Tao, X., and C. S. Gardner (1993), Heat flux observations in the mesopause region above Haleakala, *Geophys. Res. Lett.*, *22*(20), 2829–2832.

Walterscheid, R. L. (1981), Dynamical cooling induced by dissipating internal gravity waves, *Geophys. Res. Lett.*, *8*(12), 1235–1238.

Weinstock, J. (1983), Heat flux induced by gravity waves, *Geophys. Res. Lett.*, *10*(2), 165–167.

C. S. Gardner and A. Z. Liu, Department of Electrical and Computer Engineering, University of Illinois at Urbana-Champaign, 308 CSRL, 1308 West Main Street, Urbana, IL 61801, USA. (liuzr@uiuc.edu)